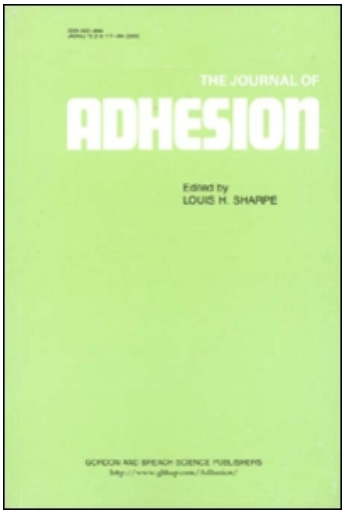

The Journal of Adhesion

Publication details, including instructions for authors and subscription information:
http://www.informaworld.com/smpp/title~content=t713453635

Interface Contributions to Localized Heating of Dielectric Thin Films

J. C. Lambropoulos[ab]; S. S. Hwang[a]
[a] Department of Mechanical Engineering, University of Rochester, Rochester, NY, USA [b] Laboratory for Laser Energetics, University of Rochester, Rochester, NY, USA

To cite this Article Lambropoulos, J. C. and Hwang, S. S.(1998) 'Interface Contributions to Localized Heating of Dielectric Thin Films', The Journal of Adhesion, 67: 1, 37 — 68
To link to this Article: DOI: 10.1080/00218469808011098
URL: http://dx.doi.org/10.1080/00218469808011098

J. Adhesion, 1998, Vol. 67, pp. 37–68
Reprints available directly from the publisher
Photocopying permitted by license only

Interface Contributions to Localized Heating of Dielectric Thin Films*

J. C. LAMBROPOULOS[a,b,**] and S.-S. HWANG[a]

[a]*Department of Mechanical Engineering;*
[b]*Laboratory for Laser Energetics, University of Rochester, Rochester, N.Y. 14627, USA*

(Received 1 October 1996; In final form 20 January 1997)

Measurements of the thermal conductivity of thin dielectric films in the last ten years have established that thin film thermal conductivity may be much lower than that of the corresponding bulk solid, by as much as two orders of magnitude, and that significant interfacial thermal resistance may be present along the film/substrate interface. We review such measurements of thin film thermal conductivity and interfacial thermal resistance, and use the heat conduction equation to determine their implications for the localized heating of thermally anisotropic thin films bonded to substrates. It is found that for surface heating an equivalent isotropic film can be established and that the presence of large interfacial thermal resistance leads to a strong dependence of film thermal conductivity on film thickness, especially for thin films. A microscopic model of the film/substrate interface is used to establish the dependence of the interfacial thermal resistance on porosity along the interface.

Keywords: Thin films; thermal conductivity; interface; thermal resistance; porosity; anisotropy

1. INTRODUCTION

The thermal conductivity of thin films may be much lower than the thermal conductivity of the corresponding bulk solids, and a significant interfacial thermal resistance may develop along the film/substrate interface. It is clear that in many instances bulk thermal conductivity

*Presented at the Symposium on *Fundamentals of Adhesion and Interfaces* at the Fall Meeting of the American Chemical Society in Orlando, Florida, USA, August 25–28, 1996.

**Corresponding author.

values are not appropriate when the removal or deposition of heat in thin films is a consideration [1, 2].

The removal of heat in layered microstructures is of importance in many electronic, optical, and optoelectronic devices. Examples are laser diodes, transistors and integrated circuits, magneto-optical recording media, and multilayer dielectric thin film laser mirrors. The removal of heat generated within these layered structures has become more severe recently due to the increase in speed of electronic devices and the emergence of high-power, short-pulse lasers. Below we briefly summarize measurements of thin dielectric film thermal conductivity. See Goodson and Flik [3], Duncan and Peterson [4], or Carpenter [5] for critical reviews of measurement techniques.

Decker *et al.* [6] reported the measurement of thermal conductivity of free-standing thin films of SiO_2 and Al_2O_3. Values were found to be one or two orders of magnitude lower than those for the corresponding bulk materials. The authors attributed this difference to the unique microstructure of dielectric thin films, which prevents them from exhibiting bulk-like properties. When deposited with physical deposition methods like sputtering or evaporation, these films are best described as somewhat inhomogeneous, anisotropic, and either polycrystalline or amorphous. Columnar growth is often observed. These films may also contain voids, pinholes, and nodular defects, which reduce the density and integrity of the film. The result is a reduced phonon mean free path and lower thermal conductivity.

More recently, Guenther and McIver [7] have discussed the implications of low film thermal conductivity for the laser damage resistance of thin dielectric films, which occurs when an absorbing inclusion embedded within a non-absorbing matrix (in this case the matrix is identified with the film) is excessively heated. The value of the critical energy density at damage depends on the thermal properties of the host material surrounding the inclusion. Although the heat capacity and density of optical thin films are close to the properties of the bulk solids [6], this is not the case for the thermal conductivity which, being considerably lower for thin films, leads to lower values of the damage threshold energy densities. In a 1990 review of X-ray lithography, Maldonado [8] stressed the importance of high thermal conductivity, high hardness, and high stiffness for the mask used to absorb X-rays. Thus, models that account for thermal transport in thin film

structures may have no predictive value if they employ bulk thermal conductivity data.

A brief survey of the current literature is given below. It reveals a strong interest in the thermal conductivity of thin layers, and a relative lack of thermal conductivity data for thin metal, polymer, and dielectric films. This survey does not include all film thermal conductivity measurements to date; it merely shows the necessity of measuring and understanding the range of thin film thermal conductivity for a large variety of technical applications.

Current optical recording technologies involve laser marking of thin organic or metal films, laser-heating induced local phase changes, and thermomagnetic recording. Laser marking is a melt/ablate process, and thermomagnetic recording involves a change in the direction of magnetization in a film. All involve absorption of laser radiation to bring a local area of the film above some threshold energy per unit volume, where the writing process occurs. Bartholomeusz [9] addressed both the uncertainty in thermal conductivity data and the lack of knowledge regarding resistance to heat flow at film-substrate interfaces. Various estimates for thin film thermal conductivity in magneto-optical recording have been discussed by Nakagawa *et al.* [10]. In their finite element analysis of blister formation and thermal stress in optical storage media, Evans and Nkansah [11] and Nkansah and Evans [12] used assumed values for the thermal conductivities of a 100-nm dye-polymer layer (0.2 $W\ m^{-1}\ K^{-1}$) and a 30-nm tellurium layer (1.5 $W\ m^{-1}\ K^{-1}$). Both were taken from the literature for bulk solids.

Decker's technique [6] included the application of thermocouples to free-standing films. Ono *et al.* [13] developed a technique for measuring the thermal conductivity of diamond films parallel to the film surface by depositing the film on a Si substrate, dissolving the substrate, applying a black paint to the front and rear surfaces of the free-standing film sample and measuring the temperature variation along the free standing film with a thermograph. Transverse temperature variations were neglected. A reoccurring problem with this technique was that the brittle film samples often broke. Tai *et al.* [14] developed a complex silicon microbridge structure to evaluate the thermal conductivity parallel to the film surface of LPCVD polycrystalline silicon films that were 1.5 μm thick. Saenger [15] used an interferometric calorimetric method to measure thin film diffusivity of

5 μm and 10 μm thick polyimide polymer films bonded to optically-transparent glass substrates. The author constructed special surface and subsurface coatings (made of Au and Cr, respectively) to deposit, heat, and reflect a probe beam properly from the sample film. The author's technique required a displacement to be measured, which was on the order of a few angstroms. Saenger's motivation was the search for improved nondestructive methods for studying thermal properties of thin films.

There are other complex optical approaches, for example the thermographic laser calorimeter [16], which employed the heating of the free film surface by a laser beam and the recording of the infrared radiation of the sample. When applied to free-standing films, such techniques do not allow the estimation of any interfacial thermal properties, such as the interfacial thermal resistance, which are expected to become increasingly important as the films become thinner.

Cahill, Fischer, Klitsner, Swartz and Pohl [17] have reviewed several techniques for measuring thermal conductivity in films with thicknesses ranging from angstroms to millimeters. For thicknesses less than 10 μm, they deposited two narrow metal strips along the film substrate interface. One strip was resistively heated, and the other strip was used as a thermometer. These authors measured the thermal conductivity of thin glass films, and they observed that the presence of a thin amorphous SiO_2 layer (with thickness in the range 7 to 115 nm) on various substrates greatly increased the interfacial thermal resistance. They found that at low temperatures the thermal conductivity of the glass film is considerably lower than that of bulk amorphous SiO_2.

Brotzen, Loos and Brady [18] measured the thermal conductivity of thin SiO_2 films deposited by chemical vapor deposition on single-crystal Si substrates, by depositing a thin Al strip on top of the film. The Al strip was heated resistively, and the temperature difference between the strip and a heat sink on which the Si substrate rested was measured. Brotzen *et al.* [18] found that the thermal conductivity of the SiO_2 films was a strong function of the film thickness (at 100°C, the thermal conductivity of the films ranged from 0.045 W m^{-1} K^{-1} to 0.22 W m^{-1} K^{-1} to 0.40 W m^{-1} K^{-1} as the film thickness varied from 0.1 to 0.7 to 1.4 μm) and that a considerable interfacial thermal resistance developed along the film/substrate interface. For comparison, we mention that Ristau and Ebert [16] measured the room temperature

thermal conductivity of 1, 2 and 3 μm thick SiO_2 films to be 0.1 W m^{-1} K^{-1}; Schafft *et al.* [19] used resistive heating methods to find 0.68 and 0.97 W m^{-1} K^{-1} for SiO_2 films of 1.74 and 3.04 μm thickness, respectively, while Decker *et al.* [6] found 0.17 W m^{-1} K^{-1} for 1.05 μm thick electron-beam evaporated SiO_2 films and 0.28 W m^{-1} K^{-1} for 0.5 μm thick sputtered SiO_2 films. It is interesting to note that the measurements of Schafft *et al.* [19], performed in the range 27 to 255°C, showed that the thermal conductivity of the films decreased with increasing temperature, thus resembling the temperature dependence of the thermal conductivity of crystalline quartz rather than fused silica whose conductivity is an increasing function of temperature [20].

Griffin *et al.* [21, 22] have discussed in detail the thickness dependence of the thin film thermal conductivity for various dielectric thin films sputtered or otherwise deposited on substrates. Their work shows clearly that the observed thickness dependence is due to the presence of a strong interfacial thermal resistance along the film/substrate interface. For thermally-grown SiO_2 films (Cahill and Allen [23] for film thickness of 0.5–2 μm; Goodson *et al.* [24] for film thickness of about 0.3 μm) the thin film thermal conductivity was found to be similar to that for bulk fused silica.

More recently, Cahill and Allen [17] measured with the 3ω method [23] the thermal conductivity of sputtered SiO_2 and TiO_2 coatings with 1–2 μm thickness deposited on Si, and observed lower values than for bulk-like similar solids. Lee *et al.* [25] used the same method for sputtered SiO_2, Al_2O_3 (amorphous), TiO_2, MgO, and HfO_2 (nanocrystalline with grain size 4–20 nm) films of thickness 0.5–2 μm. They found that the amorphous films had low thermal conductivity (1–1.6 W m^{-1} K^{-1}) comparable with that of amorphous bulk solids. The nanocrystalline films had behavior intermediate to amorphous and single-crystal bulk solids, although the value for MgO films was lower than the thermal conductivity of the bulk crystal by an order of magnitude. In this technique, the contributions from the interface were not separated from the measured thermal conductivity of the thin film.

Photothermal deflection techniques also can be used to measure the thermal conductivity of thin films. Kuo *et al.* [26] have measured the interfacial thermal resistance between thin films of amorphous Si (with

thickness from 0.25 to 1.8 μm) deposited on single-crystal Si substrates. Kuo's technique did not involve any contact with the film's free surface, but relied on the local swelling in the surface of the film when a transient laser beam of known power illuminated the surface. By using the technique of Lambropoulos *et al.* [1] to extract the film thermal conductivity and interfacial thermal resistance from the measured effective thermal conductivity, Kuo *et al.* [26] found that when the Si films were deposited on the as-received Si substrates, the interfacial thermal resistance was approximately 0.6 mm^2 K/W. When the Si substrate was cleaned with an ion beam before film deposition, the interfacial thermal resistance dropped to about 0.2 mm^2 K/W. In both cases of Si films, the film thermal conductivity was found to be about 5.5–6 W m^{-1} K^{-1} for film thicknesses in the range 0.2 to 1.8 μm. For bulk single-crystal Si, the thermal conductivity is 150 W m^{-1} K^{-1}. For comparison, the thermal resistance of a 100 nm thick layer of amorphous SiO_2 (with thermal conductivity of, say, 1 W m^{-1} K^{-1}) would be 0.1 mm^2 K/W. It is worth noting that the reduced thermal conductivity Si films had lower laser damage thresholds [27]. Observations on interfacial thermal resistance for metal/epoxy interfaces have been made by Matsumoto *et al.* [28].

It is, thus, clear that the interfacial thermal resistance between a film and a substrate may be considerable [29]. The existence of an interfacial thermal resistance implies that the temperature is not continuous across the film/substrate interface, and that the amount of temperature discontinuity is linearly related to the power flux per unit area through the interfacial thermal resistance. For example, the measurements of Lambropoulos *et al.* [1] on a wide variety of oxide and fluoride films with thickness in the sub-μm range may be as large as 3 mm^2K/W when deposited on single crystal Si or sapphire substrates. There are cases, however, when the interfacial thermal resistance is much lower. For example, the analysis of the data for AlN [30] or for the rare-earth transition-metal amorphous films studied by Shaw-Klein *et al.* [31] showed that the interfacial thermal resistance was several orders of magnitude lower than the values quoted above.

Reichling *et al.* [32] used high frequency photothermal reflectivity and displacement techniques to measure the thermal conductivity of several dielectric thin films which were coated with a thin Au layer. For 1 μm thin films deposited on BK7 glass substrates, these authors

found a significant reduction of the film thermal conductivity as compared with the bulk value. SiO_2, ZrO_2, and Ta_2O_5 films were found to have lower thermal conductivities than bulk materials. It is interesting to note that for Al_2O_3 films, Reichling *et al.* [32] concluded that the extracted film conductivity (150 W m^{-1} K^{-1}) was significantly higher than that of bulk Al_2O_3 (about 30 W m^{-1} K^{-1}). Mirage techniques have been used by Wu *et al.* [33, 34] to measure thin film thermal conductivity. Their measurements confirm the reduced thin film thermal conductivity.

Swimm [35] has used a similar technique relying on the temperature-induced modulation of the surface reflectance of a sample. This technique requires that a thin metal foil be deposited on top of the film (Swimm used Ni foils). For 0.7 μm silica films on fused silica substrates, Swimm concluded that the thermal diffusivity of the silica coating was reduced relative to the silica substrate by a factor of no more than about 1.5, and that the thermal resistance between the metal foil/silica film/silica substrate interfaces was no greater than about 0.2 mm^2 K/W.

Another method of measuring the thermal conductivity of thin films is the thermal comparator, a rapid, non-destructive and inexpensive technique [1, 36]. The thermal comparator was originally developed for the measurement of the thermal conductivity of bulk solids. A comprehensive review has been published by Powell [37]. In the thermal comparator technique, what is measured is the effective thermal conductivity of the film with contributions from the film itself and the film/substrate interface. Upon further assuming that the film conductivity is independent of film thickness over the range of measured film thicknesses, the film conductivity can be calculated.

In technical applications involving the dissipation of heat in thin film/substrate assemblies, it is not the film thermal conductivity that governs the thermal behavior of the film, but rather the effective conductivity which includes contributions from the film and from the film/substrate interface, and possibly from the substrate itself. In many instances, for example when the thermal conductivity of the film is much lower than that of the substrate, and the film thickness is much lower than the lateral extent of the area parallel to the film over which heat flows into the film, and the interfacial thermal resistance is much lower than the thermal resistance of the substrate, then the contributions from the film and the

film/substrate interface may be added, as will be shown later in this paper.

Film thermal conductivity may be anisotropic due to microstructural features related to the deposition process, or due to the crystallography of the film. The columnar microstructure, often observed in thin films (Movchan and Demchishin [38], Thornton [39, 40], Messier [41]), is expected to make the thermal conductivity anisotropic, so that the thermal conductivity in the film plane (denoted by "$\parallel$") may be quite different from that normal to the plane of the film (denoted by "$\perp$"). Shaw-Klein *et al.* [31] have measured the thermal conductivity of sputtered amorphous films of rare-earth transition metals used in magneto-optic recording (film thickness in the range 0.25–1 μm, fused silica substrates). When the films were deposited at low pressures, SEM analysis showed that the film microstructure did not exhibit any significant anisotropy, and measurement of the in-plane ($k_\parallel$) and out-of-plane ($k_\perp$) thermal conductivities showed that the film was approximately isotropic with $k_\parallel/k_\perp = 0.7$. At higher deposition pressures, the films exhibited the characteristic columnar microstructure, and a significant anisotropy in the thermal conductivity developed, with $k_\parallel/k_\perp$ approximately equal to 0.07.

In the work of Shaw-Klein *et al.* [31] both $k_\parallel$ and $k_\perp$ were measured in the same samples. The in-plane thermal conductivity was determined by first measuring the electrical in-plane resistivity and converting to electronic thermal conductivity *via* the Wiedemann-Franz law [42]. The phonon contribution to the thermal conductivity was estimated by using the Peierls model for thermal conductivity of dielectric solids [43, 44] and added to the electronic contribution to yield $k_\parallel$. The thermal conductivity normal to the plane of the film, $k_\perp$, was measured by the thermal comparator method.

The thermal anisotropy may be also due to the anisotropic crystallography of the film itself. The data of Hagen *et al.* [42] on the thermal conductivity of bulk $Y_1Ba_2Cu_3O_{7-\delta}$ showed that at room temperature the thermal conductivity along the *ab* planes was in the range of 8 to 10 W m^{-1} K^{-1}, while it was only 1–2 W m^{-1} K^{-1} along the *c* direction. Thus, a film deposited with the *c*-axis normal to the film/substrate interface would be expected to have thermal anisotropy with $k_\perp \ll k_\parallel$. For example, Shaw-Klein *et al.* [45, 53] have recently measured the thermal conductivity of superconducting $Y_1Ba_2Cu_3O_{7-\delta}$ films with

thickness in the range 0.25 to 1 μm and deposited on single crystal MgO substrates. It was found that both $k_{\parallel}$ and $k_{\perp}$ were considerably lower than the corresponding bulk single-crystal values, and that a significant anisotropy existed in the thin films with $k_{\perp} \ll k_{\parallel}$.

The discussion above, summarizing some recent measurements of thin film thermal conductivity, leads to the conclusion that the presence of interfacial thermal resistance between the film and the substrate and the thermal anisotropy in the film may be significant factors. In this paper, we determine the apparent thermal conductivity of a half-space coated by a thermally-anisotropic thin film when there is an interfacial thermal resistance between the film and the substrate, and we discuss some microstructural contributions to the interfacial thermal resistance and the film thermal anisotropy.

2. THERMAL RESISTANCE OF A HALF-SPACE

We first consider the axisymmetric half-space $z > 0$, of thermal conductivity k_{app}, where r, z are cylindrical coordinates. The surface $z = 0$ is heated, so that

$$-k_{app}\frac{\partial T}{\partial z} = Q\begin{cases} f(r) & \text{for } r \leqslant a \\ 0 & \text{for } r > a \end{cases} \quad \text{at } z = 0 \tag{1}$$

where Q is the total power entering the half-space, $f(r)$ gives the spatial distribution of the power flux, and a is the thermal contact radius. Far from the heated area, the temperature decays to ambient. The temperature $T(r, z)$ is determined under steady-state conditions by using Hankel transforms of order zero. The temperature is then

$$T(r, z) = \frac{Q}{k_{app}}\int_0^{\infty} F(\xi)\exp(-\xi z)\,J_0(\xi r)\,d\xi \quad F(\xi) = \int_0^a f(r)\,J_0(\xi r)\,r\,dr \tag{2}$$

where $F(\xi)$ is the zero order Hankel transform of the spatial distribution function, $f(r)$.

Carslaw and Jaeger [46] have analyzed heat flow from a circular region of radius a on the surface of a half-space of uniform thermal conductivity. They defined the thermal constriction as the ratio of

temperature increase over the circular region of radius a to the power flowing through that region (see also Dryden [47]). We define the thermal resistance, R, in a slightly different manner, namely as the ratio of the average temperature change over the circular region of the surface of radius a to the average power flux, $Q/(\pi a^2)$, over that area. Thus,

$$R = \frac{(\pi a^2)^{-1} \int_0^a T(r, z=0)\, 2\pi r\, dr}{Q/(\pi a^2)} \tag{3}$$

By further using Eq. (2) for the temperature distribution, and changing the order of integration, we find that

$$R = 2\pi \frac{a}{k_{\text{app}}} \int_0^a \frac{F(\xi)}{\xi} J_1(\xi a)\, d\xi \tag{4}$$

To further determine the thermal resistance, R, we need the precise distribution of the power flux, $f(r)$, over the heated area. We assume that the spatial distribution of the power flux is given by

$$f(r) = \frac{(1+\mu)(a^2 - r^2)^{\mu}}{\pi a^{2(1+\mu)}} \tag{5}$$

where μ is an exponent with typical values between $-1/2$ and 1. Now the function $F(\xi)$ of Eq. (2) can be found (see Oberhettinger [48]) as

$$F(\xi) = \frac{(1+\mu)\,\Gamma(1+\mu)}{\pi} \frac{J_{1+\mu}(a\xi)}{(a\xi)^{1+\mu}} 2^{\mu} \tag{6}$$

Substitution into Eq. (4) allows the evaluation of the thermal resistance, R (Gradshtyn and Rhezhik, 1980), as

$$R = \frac{a}{k_{\text{app}}} \frac{(1+\mu)\,\Gamma(1+\mu)\,\Gamma(2+\mu)}{\Gamma\left(\frac{5}{2}+\mu\right)\Gamma\left(\frac{3}{2}+\mu\right)} \tag{7}$$

Figure 1 shows the dependence of the dimensionless thermal resistance, Rk_{app}/a, on the exponent μ. It is seen that for μ in the range $-1/2$ to 1 the dependence of R on μ is rather weak. Based on this observation, and in agreement with the analysis of Dryden [47], we will assume that $\mu = -1/2$ is an adequate description of the heat flux profile along $z = 0$.

3. THIN FILM ANISOTROPY AND INTERFACIAL THERMAL RESISTANCE

Consider a film of thickness H bonded to a semi-infinite substrate as shown in Figure 2. The film is thermally anisotropic, with thermal conductivity, $k_\perp$, normal to the film-substrate interface, and thermal conductivity, $k_\parallel$, parallel to the interface. The substrate has the isotropic thermal conductivity k_2. Under steady-state conditions, the

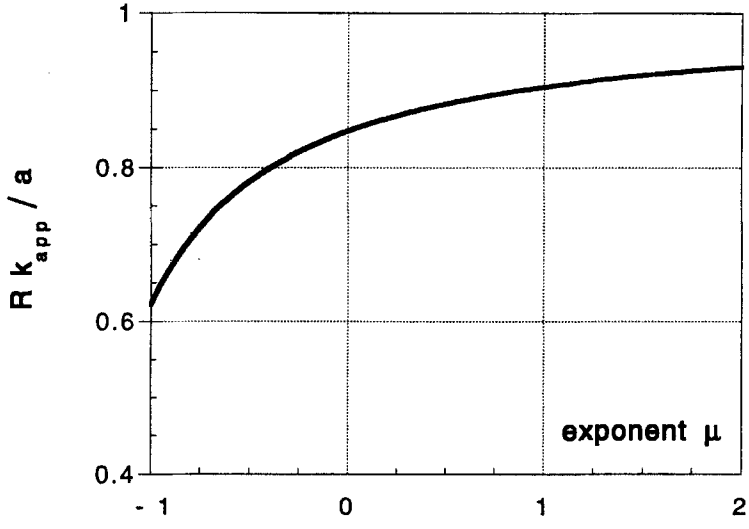

FIGURE 1 The dimensionless thermal resistance of a half-space *vs.* the exponent μ describing the heat flux in the surface of the half-space where the heat flux is proportional to $(a^2 - r^2)^\mu$ for $r < a$.

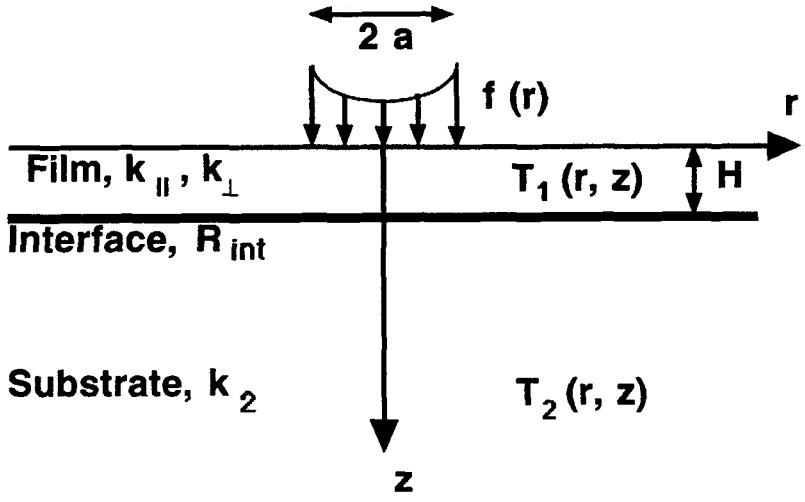

FIGURE 2 A thermally anisotropic thin film is bonded to an isotropic semi-infinite substrate *via* an interface with interfacial thermal resistance R_{int}. The film is heated under steady-state conditions *via* a surface spot of radius a (the heat flow radius).

temperature, $T_1(r, z)$, in the film and $T_2(r, z)$ in the substrate satisfy

$$k_{\parallel}\left(\frac{\partial^2 T_1}{\partial r^2}+\frac{1}{r}\frac{\partial T_1}{\partial r}\right)+k_{\perp}\frac{\partial^2 T_1}{\partial z^2}=0 \quad \text{in the film } (0\leqslant z\leqslant H)$$
$$k_2\left(\frac{\partial^2 T_2}{\partial r^2}+\frac{1}{r}\frac{\partial T_2}{\partial r}+\frac{\partial^2 T_2}{\partial z^2}\right)=0 \quad \text{in the substrate } (H\leqslant z\leqslant \infty) \tag{8}$$

The boundary conditions along the film-substrate interface $z = H$ are

$$k_{\perp}\frac{\partial T_1}{\partial z}=k_2\frac{\partial T_2}{\partial z}, \quad k_2\frac{\partial T_2}{\partial z}+\frac{T_1-T_2}{R_{\text{int}}}=0 \tag{9}$$

where the first of Eqs. (9) expresses the continuity of power flux, and the second approximates the temperature discontinuity at the interface which is proportional to the interfacial thermal resistance, R_{int}. Notice that if $R_{int} = 0$, then the temperature is continuous at the interface. If $R_{int} \to \infty$ then the interface is thermally insulated. In the case of the isotropic film without any interfacial thermal resistance, the problem was solved by Dryden [47].

For a first principles calculation of R_{int} and its dependence on temperature, especially at low temperatures (typically less than 100–200 K), refer to the work of Cahill *et al.* [23] and Swartz and Pohl [29]. For a fractal analysis of the contact conductance between two rough surfaces, see Majumdar and Tien [50]. For the time being, R_{int} will be treated as a phenomenological parameter describing the film/substrate interface.

At the free surface of the film ($z = 0$) it is assumed that there is the prescribed power flux

$$k_\perp \frac{\partial T_1}{\partial z} = \begin{cases} Qf(r) & 0 < r < a \\ 0, & a < r \end{cases} \qquad z = 0 \tag{10}$$

Following the analysis in the previous section, the current problem is also solved by using Hankel transforms of order zero. The thermal resistance, defined *via* Eq. (3), is found as

$$R = \frac{2\pi a}{\sqrt{k_\parallel k_\perp}} \int_0^\infty \frac{F(\xi)}{\xi} J_1(\xi a)\, G\left(\xi a, \frac{\sqrt{k_\parallel k_\perp}}{k_2}, \beta \frac{H}{a}, \rho\right) d\xi \tag{11}$$

where the degree of anisotropy, β, and dimensionless interfacial thermal resistance, ρ, are

$$\beta \equiv \sqrt{k_\parallel / k_\perp} \qquad \rho \equiv \frac{R_{int} k_2}{a} \tag{12}$$

The dimensionless kernel, $G(\xi, \kappa, t, \rho)$, is due to the presence of the film. In the absence of any film $G = 1$. The kernel, G, is

$$G(\xi, \kappa, t, \rho) \equiv \frac{1 - e^{-2\xi t} + \kappa(1 + e^{-2\xi t})(1 + \xi\rho)}{1 + e^{-2\xi t} + \kappa(1 - e^{-2\xi t})(1 + \xi\rho)} \tag{13}$$

On the other hand, if the coated half-space were homogeneous with an apparent thermal conductivity k_{app}, the thermal resistance would be given by Eq. (4). Equating (4) to (11) we find that the apparent

thermal conductivity, k_{app}, is

$$\frac{k_{app}}{\sqrt{k_{\parallel}k_{\perp}}} = \frac{\int_0^\infty \frac{F(\xi)}{\xi} J_1(\xi a)\, d\xi}{\int_0^\infty \frac{F(\xi)}{\xi} J_1(\xi a)\, G\left(\xi a, \frac{\sqrt{k_{\parallel}k_{\perp}}}{k_2}, \beta\frac{H}{a}, \rho\right) d\xi} \tag{14}$$

Eq. (14) clearly shows that the original anisotropic film, of thickness H and thermal conductivity $k_{\perp}$ normal to the film-substrate interface, and thermal conductivity $k_{\parallel}$ parallel to the interface, is equivalent to an isotropic film with equivalent thickness H_{eq} and equivalent thermal conductivity k_{eq} given by

$$H_{eq} = \beta H = \sqrt{\frac{k_{\parallel}}{k_{\perp}}}\, H, \qquad k_{eq} = \sqrt{k_{\parallel}k_{\perp}} \tag{15}$$

It is the apparent thermal conductivity, k_{app}, that is often measured directly, for example by the thermal comparator [1, 30, 31] or by the photothermal displacement technique [26]. Clearly, the apparent thermal conductivity, k_{app}, of the coated substrate has contributions from the film, the film/substrate interface, and the substrate, and also depends on the heat flow radius, a. The substrate thermal properties, the film thickness, H, and the heat flow radius, a, can be independently measured or estimated, so that Eq. (14) essentially relates the film thermal conductivity, k_{eq}, to the measured k_{app} and to the interfacial thermal resistance, ρ, which characterizes the film/substrate interface.

As an example of the effect of a film on the apparent thermal conductivity of a coated substrate, we consider the case when the power flux has the inverse square root singularity, $\mu = -1/2$, in Eq. (5). The results are shown in Figures 3A–C, where the horizontal axis is the dimensionless equivalent film thickness, H_{eq}/a, with H_{eq} related to the actual film thickness, H, *via* Eq. (15), and the vertical axis is the apparent thermal conductivity of the coated substrate (with contributions from the film, the film/substrate interface, and the substrate) measured with respect to the thermal conductivity, k_2, of the substrate. Results for $\rho = 0.01$ (not shown) were practically indistinguishable from those for $\rho = 0.1$.

Typical values of the dimensionless interfacial thermal resistance, ρ, are in the range 0.01 to 3. For example, the work of Kuo *et al.* [26]

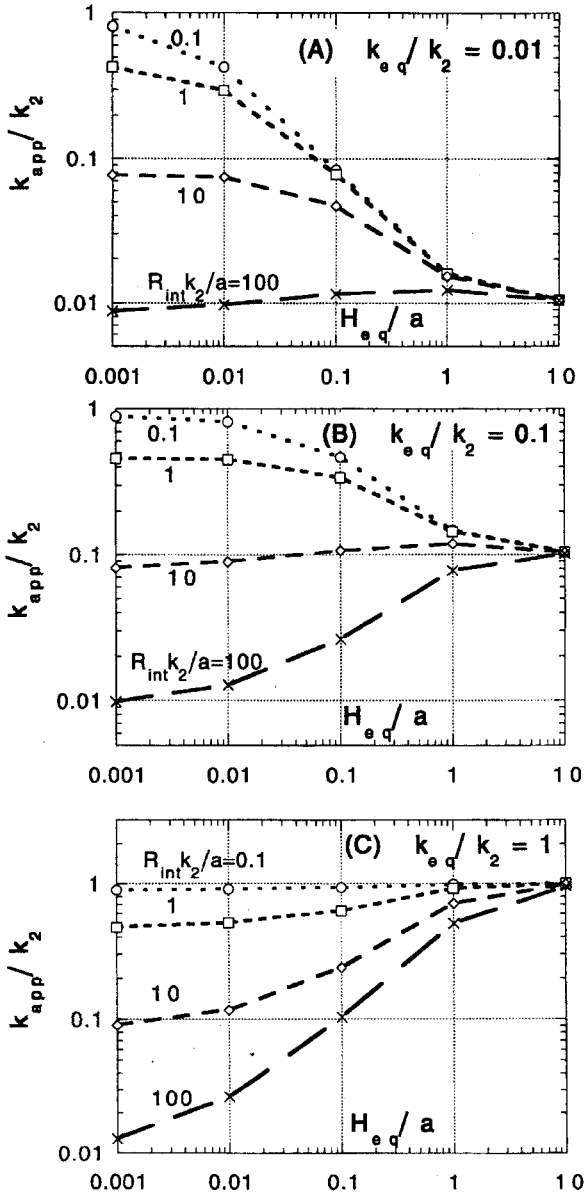

FIGURE 3 (A)–(C) The dependence of the apparent thermal conductivity, k_{app}, of a coated substrate on the equivalent film thickness and the dimensionless interfacial thermal resistance, ρ. The apparent thermal conductivity, k_{app}, consists of contributions due to the film, the film/substrate interface and the substrate.

on Si films had $R_{int} = 0.5$ mm^2 K/W and $a = 30$ μm on Si substrates, leading to $\rho = 2.5$; the work of Reichling *et al.* [32] on silica films on BK7 glass substrates ($k_2 = 1.1$ W m^{-1} K^{-1}, $a = 30$ μm) with the same value of R_{int} as Kuo *et al.* [26] leads to $\rho = 0.01$.

Figures 3A–C show that for thick films, as $H_{eq}/a \to \infty$, then $k_{app} \to k_{eq} \equiv (k_\parallel k_\perp)^{1/2}$, *i.e.* the effect of the substrate increasingly disappears. The effect of the non-dimensional interfacial thermal resistance, ρ, is also very small when $H_{eq} \gg a$, implying that thick coatings, as expected, are not sensitive to the presence of the interface.

For thin films (say, $H_{eq}/a \leqslant 0.1$), on the other hand, the apparent thermal conductivity, k_{app}, is a strong function of the interfacial thermal resistance, ρ. For very thin films ($H_{eq}/a \leqslant 0.01$), k_{app}/k_2 depends weakly on k_{eq}/k_2 for insulating films ($k_{eq}/k_2 \leqslant 0.1$) and depends mainly on the non-dimensional thermal resistance, ρ. Also for insulating films, and for small values of ρ (say, $\rho \leqslant 1$), k_{app} is near the substrate's k_2 and the presence of the film leads to a perturbation from k_2. In this case, k_{app}/k_2 depends weakly on ρ and changes by not more than a factor of 2 for all film thicknesses as ρ changes from 0 to 1. However, for large values of ρ, k_{app}/k_2 is approximately equal to $1/\rho$, or $k_{app} = a/R_{int}$, so that the measured apparent conductivity, k_{app}, is dominated by the presence of the interface.

As discussed in the introduction, thin films may have much lower thermal conductivities compared with the corresponding bulk solids, so that Figures 3A–B are applicable to such thin films deposited on substrates with much higher thermal conductivity (for example, at room temperature Si substrates with $k_2 = 150$ W m^{-1} K^{-1}, sapphire substrates with $k_2 = 35$ W m^{-1} K^{-1}, or MgO substrates with $k_2 = 35$ W m^{-1} K^{-1}). For substrates with lower thermal conductivity (for example fused SiO_2 or other optical glasses with k_2 about 1–2 W m^{-1} K^{-1} at room temperature) Figure 3C is applicable.

For the case of small interfacial thermal resistance ($\rho \ll 1$) and thin films ($H_{eq} \ll a$), Eq. (14) with $\mu = -1/2$ leads to the asymptotic result

$$\frac{k_{app}}{k_2} = 1 - \frac{4}{\pi} t \frac{1-\kappa^2}{\kappa} + \frac{32\sqrt{2}}{3\pi} t^{3/2} \frac{f_1(\kappa)}{\kappa} + O(t^{5/2})$$

$$- \rho \frac{4}{\pi} \left\{ 1 - 4\sqrt{2}\, t^{1/2} \frac{f_1(\kappa)}{\kappa^2 - 1} + 2\sqrt{2}\, t^{3/2} \frac{f_2(\kappa)}{k^2 - 1} + O(t^{5/2}) \right\} \quad (16a)$$

where we have denoted

$$t \equiv \frac{H_{eq}}{a} = \sqrt{\frac{k_\parallel}{k_\perp}}\,\frac{H}{a}, \quad \kappa \equiv \frac{k_{eq}}{k_2} = \sqrt{k_\parallel k_\perp}\,k_2 \tag{16b}$$

The functions $f_1(\kappa)$ and $f_2(\kappa)$ are shown in Figure 4. It is seen that for a thermally-insulating film with respect to the substrate ($\kappa \leqslant 1$) these functions have a small value, but they attain much larger values when the film is more conducting than the substrate. Eq. (16) clearly shows that in this limiting case of thin films with small interfacial resistance the effect of the film and of the film/substrate interface is to add a perturbation to the measured thermal conductivity, k_{app}, from the substrate thermal conductivity, k_2.

Furthermore, when $(k_\parallel k_\perp)^{1/2} \ll k_2$, the higher order terms may be neglected, so that

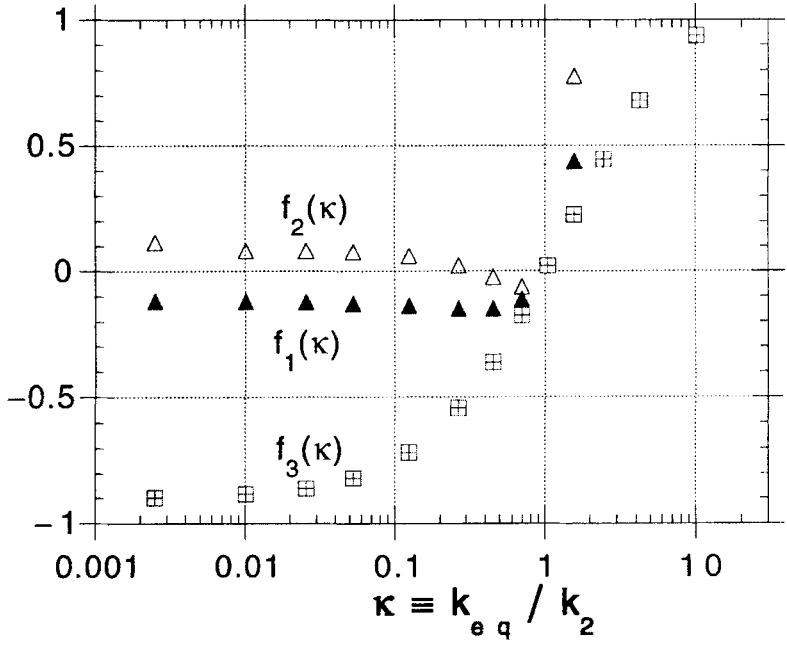

FIGURE 4 The functions f_1, f_2, and f_3 of the dimensionless variable k_{eq}/k_2. These functions enter the calculation of the apparent thermal conductivity for the case of thin films (f_1 and f_2) or thick films (f_3).

$$\frac{4}{\pi}\frac{a}{k_{app}} = \frac{H}{k_\perp} + R_{int} + \frac{4}{\pi}\frac{a}{k_2} \tag{17}$$

This equation implies that for thin, insulating films with low interfacial thermal resistance ($H_{eq} \ll a$, $(k_\parallel k_\perp)^{1/2} \ll k_2$, and $R_{int} k_2/a \ll 1$), the total thermal resistance of the coated substrate is the sum of the thermal resistance due to the film ($H/k_\perp$), the interface (R_{int}) and the substrate ($4a/\pi k_2$). Thus, if we combine the effects of the film and the film/substrate interface into a single term governed by an "effective" thermal conductivity, k_{eff}, we find

$$\frac{H}{k_{eff}} = \frac{H}{k_\perp} + R_{int} \quad \text{or,} \quad \frac{k_{eff}}{k_\perp} = \frac{\left(\frac{H}{R_{int} k_\perp}\right)}{1 + \left(\frac{H}{R_{int} k_\perp}\right)} \tag{18}$$

The result above, shown in Figure 5, indicates that for thin films the measured film conductivity increases linearly with the film thickness and decreases with the film/substrate interfacial thermal resistance. This formulation is convenient, because often the effect of the interface can not be separated from the thin film thermal conductivity, as in the work of Kuo *et al.* [26] on Si films or Brotzen *et al.* [18] and Schafft *et al.* [19] some of whose measurements on SiO_2 films were summarized in the Introduction.

On the other hand, for small interfacial thermal resistance and a thick film ($H_{eq} \to \infty$), k_{app} is conveniently measured with respect to the film thermal conductivity, $k_{eq} \equiv (k_\parallel k_\perp)^{1/2}$. The asymptotic result is

$$\frac{k_{app}}{\sqrt{k_\parallel k_\perp}} = 1 - \frac{2}{\pi t^2}\ln\frac{\kappa+1}{2} + \frac{7}{24\pi t^3} f_3(\kappa) + O(t^{-4})$$

$$- \rho\frac{2}{\pi t^2}\left\{\frac{\kappa}{\kappa^2-1}\ln\frac{\kappa+1}{2} - \frac{7}{16 t^2}\frac{\kappa}{\kappa^2-1} f_3(\kappa) + O(t^{-4})\right\} \tag{19}$$

where the function $f_3(\kappa)$ is shown in Figure 4.

In many applications one is interested primarily in thin, insulating films in which case Eq. (18) is applicable. Assuming that the film

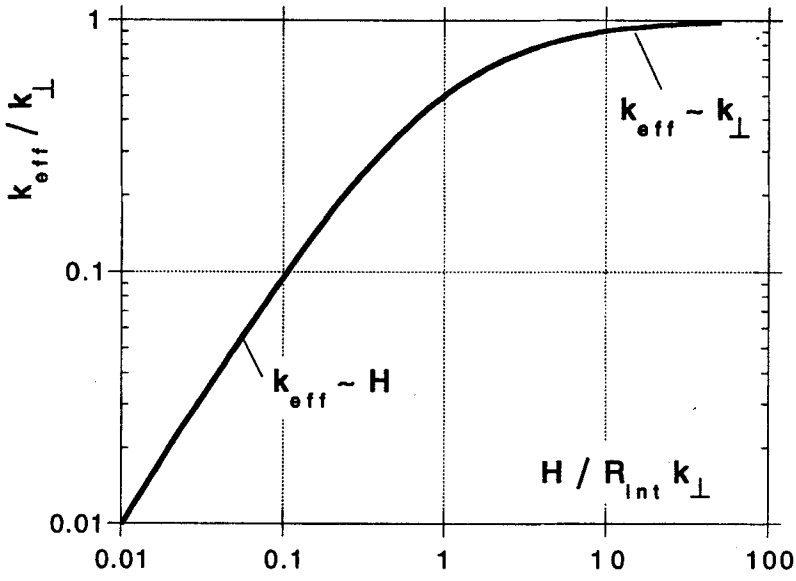

FIGURE 5 The dependence of the effective film thermal conductivity, k_{eff} (including contributions from the film and the film/substrate interface), on the dimensionless film thickness, H, for the case of small H/a, ρ, and k_{eq}/k_2. The thermal conductivity of the film material itself is $k_\perp$ in a direction normal to the film surface.

thermal conductivity, $k_\perp$, is not a function of the film thickness, H, then from the dependence of the directly-measured k_{eff} on film thickness, H, the film thermal conductivity, $k_\perp$, can be extracted by plotting H/k_{eff} *vs.* film thickness H. The slope of the resulting line is $1/k_\perp$, and the intercept is R_{int}.

Such plots are shown in Figure 6 for oxide films deposited on insulating (glass BK7) or conducting (Si) substrates, in Figure 7 for Si_3N_4 on Si, and in Figure 8 for the measurements of Kuo *et al.* [26] on amorphous Si films on Si. Table I summarizes and results of this procedure for various dielectric thin films.

Eq. (18) clearly leads to a strong variation of k_{eff} with film thickness, H, especially at small film thickness, as shown in Figure 5. We note that the reduction of k_{eff} with respect to the film value of $k_\perp$ is entirely due to the interfacial thermal resistance, and that this formulation does not account for any dependence of $k_\perp$ on film thickness, H.

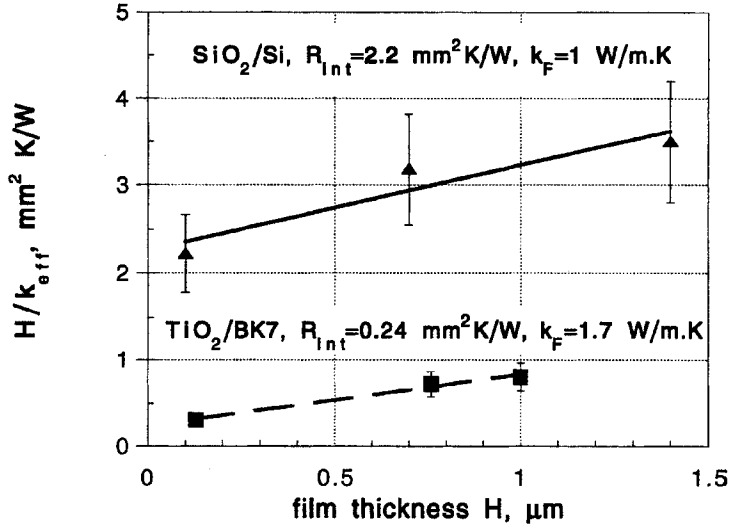

FIGURE 6 Extraction of the interfacial thermal resistance and film thermal conductivity for oxide films. Data for thermal conductivity of SiO_2 films on crystalline substrates are from Brotzen *et al.* [18], and for TiO_2 on BK7 glass from Wu *et al.* [33, 34].

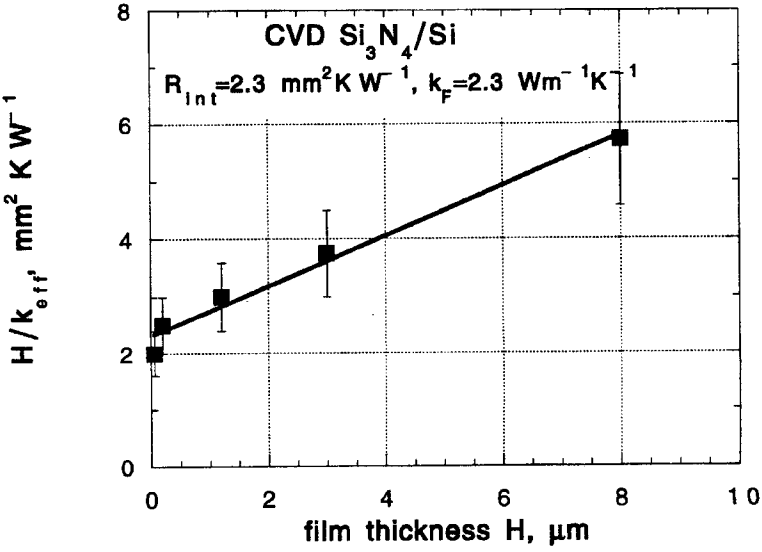

FIGURE 7 Extraction of the interfacial thermal resistance and film thermal conductivity for Si_3N_4 films deposited on crystalline Si substrates. Data on film thermal conductivity are from Griffin *et al.* [22].

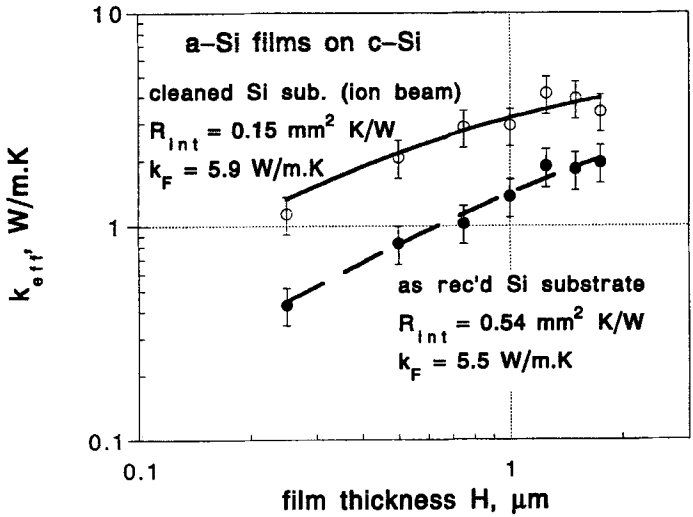

FIGURE 8 Extraction of the interfacial thermal resistance and film thermal conductivity for amorphous Si films deposited on crystalline Si substrates, based on the measurements of Kuo *et al.* [26]. The films were vacuum deposited on as-received substrates and on ion-beam-cleaned substrates.

4. DISCUSSION OF MICROSTRUCTURAL EFFECTS

We have treated in the previous Section the interfacial thermal resistance and extent of film thermal anisotropy as phenomenological parameters describing the film/substrate interface and film microstructure, respectively. We discuss below some microstructural contributions to the interfacial thermal resistance.

4a. Interface Porosity

We first consider the effect of microstructural porosity along the film/substrate interface. Continuity of temperature along the film/substrate interface is satisfied only when there is no interfacial thermal resistance. Clearly, this will be the case if no microstructural details are present along that interface.

It is well known that due to the nucleation of the thin film deposited on a substrate, the interface may have a large amount of porosity. This porosity appears to be localized near the interface in films charac-

TABLE I Summary of thin film and interfacial thermal resistance measurements for dielectric thin films. When an interfacial thermal resistance value is entered, the interface effects have been separated from the film, *i.e.* k_F is reported. Otherwise, the reported values include the contributions from the interface, *i.e.* k_{eff} is reported. Bulk thermal conductivity is at room temperature from Touloukian *et al.* [20]

Film/Substrate	*Film thickness* H *μm*	*Film thermal conductivity* k_F or k_{eff} *W/m.K*	*Bulk thermal conductivity* k_{bulk} *W/m.K*	*Interfacial thermal resistance* R_{int} *mm^2 K/W*	*Thin Film Reference*
CVD SiO_2/Si	0.1–1.4	0.67	1–11	2.1	[18]
CVD SiO_2/Si	0.008–1.7	1.5	1–11	2.1	[21]
(sputter, evap.) SiO_2/Si	1	1–0.7	1–11	–	[17]
SiO_2/BK7 glass	1	0.25	1–11	–	[32]
sputter SiO_2/Si	0.5–2	0.4–1.1	1–11	0–1.8	[1]
e-beam evap. SiO_2/Si	0.5–2	0.4–0.6	1–11	0.1–1.1	[1]
SiO_2/glass	1	0.25	1–11	–	[33]
free SiO_2	0.5–1.05	0.2–0.3	1–11	–	[6]
free Al_2O_3	1	0.04–0.25	20–46	–	[6]
anodic Al_2O_3/Al	20–100	0.5–1	20–46	–	[51]
anodic free Al_2O_3	0.14	1.6	20–46	–	[52]
sputter Al_2O_3/Si	0.5–2	1–1.6	20–46	–	[25]
Al_2O_3/Si	0.2–0.5	0.72	20–46	1.0	[1]
sputter Al_2O_3/Si	0.5–2	0.12	20–46	–	[36]
sputter TiO_2/Si	0.5–2	0.59	7–10	2.7	[1]
TiO_2/–	–	0.25–0.45	7–10	–	[33]
TiO_2/glass	0.1–1	1.7	7–10	0.24	[34]
(sputter, evap.) TiO_2/Si	1	1.5–1	7–10	–	[17]
sputter TiO_2/Si	0.5–2	1.5–5	7–10		[25]

ThO_2/Sapphire	0.2–0.4	0.67	15	0.6	[1]
HfO_2/Sapphire	0.2–0.4	0.05	0.5	–	[1]
HfO_2/glass	0.26	0.08	1.6	–	[33]
HfO_2/Si	0.5–2	1–1.5	1.6	–	[25]
ZrO_2/Sapphire	0.2–0.5	0.04	1–2	–	[1]
ZrO_2/BK7 glass	1	0.05	1–2	–	[32]
sputter Ta_2O_5/Si	0.5–2	0.12	–	–	[36]
Ta_2O_5/–		0.20–0.35	–	–	[34]
Ta_2O_5/BK7 glass	1	0.20	0.33	–	[32]
sputter MgO/Si	0.5–2	3.5–4	35	–	[25]
$YBa_2Cu_3O_{7-\delta}$/MgO	0.25–1	0.26	8–10	0.5	[53]
MgF_2/Si	0.5–2	0.6	15–30	0	[1]
MgF_2/glass	0.8–1	30	15–30	0	[33]
Si/Si (as received)	0.25–1.8	5.5	150	0.54	[26]
Si/Si (cleaned)	0.25–1.8	5.9	150	0.15	[26]
AlN/sapphire	0.15	0.5	70–180	–	[30]
AlN/quartz	0.25–1	16	70–180	–	[30]
CVD Si_3N_4/Si	0.01–10	2.0	25	2.2 (60°C)	[22]
CVD Si_3N_4/Si				~ 4 (200°C)	[22]
sputter Si_3N_4/Si	0.5–2	0.15	25	–	[36]

terized by a columnar microstructure (Messier [41]; Yang *et al.* [54]). On the other hand, growth of nodular defects at the film/substrate interface (Dubost *et al.* [55]) also contributes to a finite interfacial thermal resistance. The presence of porosity or nodular defects implies that the film/substrate interface is not to be viewed as a single plane, but instead as a diffuse region characterized by a distribution of voids or other defects.

To determine the effect of porosity on the interfacial thermal resistance, we have modeled the porous interface by examining a single cylindrical tapering grain, as shown in the insert of Figure 9. The diameter of the grain at the free film surface is D, and contact between the grain and the substrate occurs over a circle of diameter $b < D$. The height of the void is h. We assume that as $z \to \infty$ the temperature distribution is linear in z, corresponds to a constant heat flux q (power per unit area) in the $(-z)$ direction, there is no heat flow from one

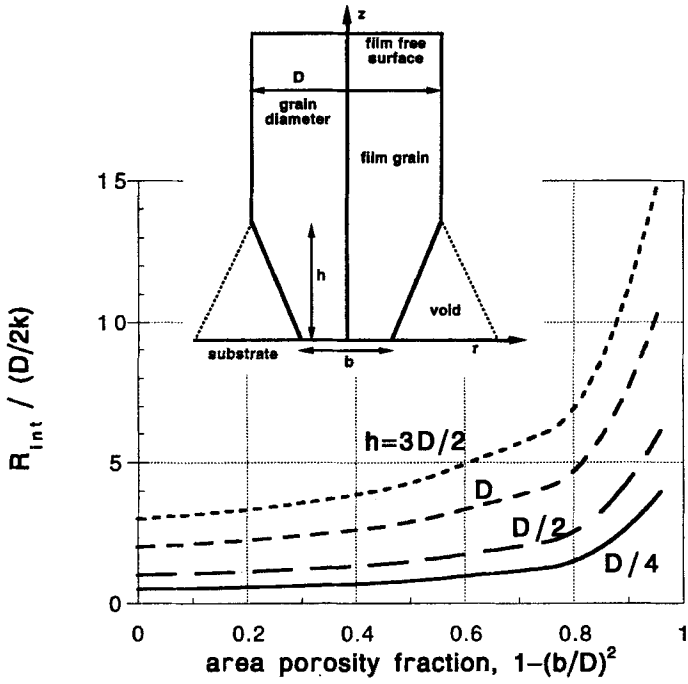

FIGURE 9 The dependence of interfacial thermal resistance on the area porosity fraction at the film/substrate interface. The insert shows the grain and void geometry.

grain to a neighboring grain, and the film is in contact with a conducting substrate so that the interface at $z = 0$ is kept at a constant temperature. We also assume that the phonon mean-free-path is smaller than any microstructural dimensions describing the void distribution, so that the usual heat conduction equation applies.

We denote by $T_0(r, z)$ the temperature distribution in the absence of any porosity so that

$$T_0(r, z) = \frac{qz}{k} \tag{20}$$

where k is the thermal conductivity of the grain material. On the other hand, in the presence of interface porosity we denote the temperature by $T(r, z)$. Porosity leads to higher temperatures in the vicinity of the film/substrate interface and this implies a higher interfacial thermal resistance.

To determine the effect of the interface porosity on the interfacial thermal resistance, we calculate the average temperature at a height z above the interface

$$T_{ave}(z) = \frac{\int_0^{D/2} T(r, z)\, 2\pi r\, dr}{\pi D^2/4} \tag{21}$$

and we can then determine the interfacial thermal resistance by

$$R_{int} = \frac{T_{ave}(z = h)}{q}, \quad R_{int,0} = \frac{T_{ave,0}(z = h)}{q} = \frac{h}{k} \tag{22}$$

This definition of the thermal resistance is identical with the definition used in Eq. (3). The first term in (22) corresponds to the temperature profile which is perturbed by the void. Notice that these contributions to the interfacial thermal resistance do not include any intrinsic thermal resistance, an example of which is the interfacial thermal resistance of two different solids brought into intimate contact through an otherwise perfect interface.

Figure 9 shows the dependence of the interfacial thermal resistance on the void geometry. The effect of area porosity fraction along the

interface, *i.e.* $1-(b/D)^2$, is strong so that the interfacial thermal resistance decreases as b/D increases. It is concluded, therefore, that a large contribution to interfacial thermal resistance may be due to the interfacial pore microstructure.

As an example, we consider the case of 10% area porosity along the interface. We then find that, depending on the void geometry as given by h/D, the interfacial thermal resistance is in the range of (0.5 to 3) $(D/2k)$. Using a typical size of column diameter, say 0.5 μm, we then find that the interfacial thermal resistance is in the range of 0.1–0.8 $mm^2\ K\ W^{-1}$ for $k = 1\ W\ m^{-1}\ K^{-1}$ (typical for SiO_2 films), and in the range of 0.4 to 2.5 $mm^2\ K\ W^{-1}$ for $k = 0.3\ W\ m^{-1}\ K^{-1}$. These values are within the approximate range of interfacial thermal resistance tabulated in Table I. We next consider the effect of porosity within the film itself.

4b. Film Porosity and Grain Boundary Structure

The density of conventionally deposited (sputtered or evaporated) thin films is often lower than that of bulk materials. The familiar columnar microstructure which often results from physical vapor deposition is well documented (Movchan and Demchishin [38]; Thornton [40, 56]; Messier [41]; Mazor [57]; Yang *et al.* [54]). Voids between the columns account for much of the decreased density. Chemical vapor deposited films (CVD) are often denser, although their dendritic growth pattern can also lead to lowered densities. Finally, sol-gel films, which originate as liquids spun or dipped onto substrates and subsequently dried, are even more porous, and may even exhibit open porosity. Messier [41] has pointed out that the microstructural features of thin films (voids, columns) can no longer be described as individual entities; instead, they must be described by distribution functions. For example, for low adatom mobility, a fractal model can be used to describe the natural clustering occurring during the aggregation of atoms.

Many models account for the effect of porosity on thermal conductivity. For example, Maxwell [58] found the conductivity of a dilute concentration (volume fraction p) of a dispersed phase of inclusions of spherical shape embedded within a continuous matrix. The effect of finite concentration for spherical dispersed phase has been considered by Brailsford and Major [59], and by Hashin and Shtrikman [60] and Budiansky [61] who used effective medium theory. Schulz [62]

has developed a general expression for the thermal conductivity of a solid containing inclusions of various shapes. The result of Schulz is applicable to the case of dispersions of spheres, or of parallel and series arrangements of the phases. Pores of shapes other than spherical have been considered by Reynolds and Hough [63], by Rocha and Acrivos [64, 65] for dilute suspensions, by Redondo and Beery [66] and by Miloh and Benvensite [67] for cracked solids.

If the porosity (volume fraction p) in the film is due to spaces between columns, randomly distributed pores may not be an accurate model. Instead, we follow Shaw-Klein [45] and treat the porosity as slabs of bulk material (columns) separated by slabs of air (porosity). Using the analogy of parallel or series resistors, $k_{\parallel}$ (parallel to the film plane, *i.e.* normal to the columns) is

$$\frac{1}{k_{\parallel}} = \frac{p}{k_{gb}} + \frac{1-p}{k_G} \tag{23a}$$

where k_{gb} is the thermal conductivity across the column grain boundaries and k_G that along the grain itself. Normal to the film (*i.e.* parallel to the columns) the result is

$$k_{\perp} = pk_{gb} + (1-p)k_G \tag{23b}$$

Columnar structures, which often result from physical vapor deposition, not only lower the thermal conductivity of the film, but also introduce anisotropic effects. Even if the columns are in contact and porosity effects discussed above are ignored, we can expect a decrease in film thermal conductivity due to the interfacial thermal resistance, R_{col}, of the column contacts. Treating the film as a composite made up of columnar grains, the anisotropic thermal conductivity is now given by

$$\frac{k(\phi)}{k_G} = \frac{\dfrac{k_{\parallel}}{k_G}}{\dfrac{R_{\text{col}}k_G}{D}\dfrac{k_{\parallel}}{k_G} + 1} \sin^2\phi + \frac{k_{\perp}}{k_G}\cos^2\phi \tag{24}$$

where D is the grain diameter, $\phi = 0$ is the direction parallel to the column (*i.e.* normal to the film), and $k_{\perp}$, $k_{\parallel}$ are functions of porosity as given by Eq. (23). Figure 10 shows the dependence of $k(\phi)/k_G$ on the

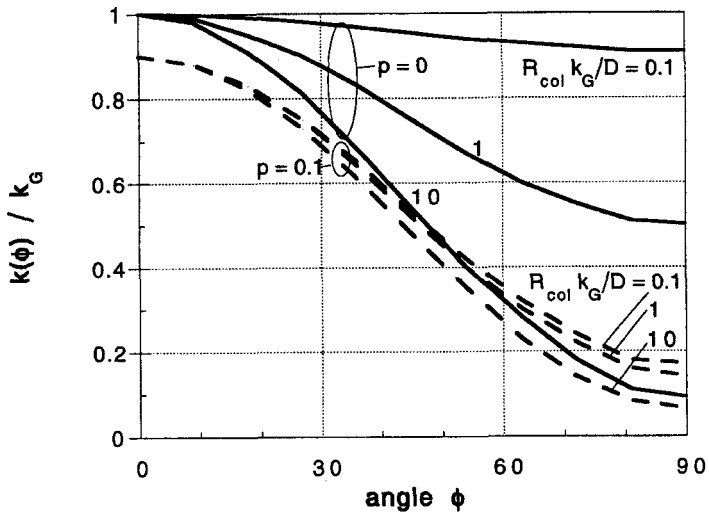

FIGURE 10 Anisotropy in the film thermal conductivity due to porosity in the film (vol. fraction p) and thermal resistance, R_{col}, between columnar grains of diameter D. The angle $\phi = 0$ corresponds to the direction normal to the film, and $\phi = 90°$ parallel to the film. The grains have thermal conductivity k_G, and the grain boundary material has $k_{gb} = 0.02\ k_G$. The solid lines are for fully-dense ($p = 0$), and the dashed lines for 10% porosity within the grains ($p = 0.1$).

angle ϕ. For no porosity, the effect of R_{col} is significant when R_{col} is of order D/k_G. As soon as the porosity takes a small non-zero value, the effect of the interfacial resistance, R_{col}, becomes small since the thermal resistance due to porosity exceeds that due to the contacts along different grains.

Although it was assumed in deriving Eq. (24) that the columns are perfectly perpendicular to the interface, this may not be necessarily so. Models of film growth suggest that the grains have a distribution of directions, and this is consistent with Messier's [41] observations and Wu *et al.*'s discussion [33, 34].

5. CONCLUSIONS

We have considered the effect of the interfacial thermal resistance along the film/substrate interface of a coated substrate at two levels.

At the continuum level, we have found the apparent thermal conductivity of a coated substrate heated over a localized area on its

surface. The effect of a thermally-anisotropic film is to behave like an equivalent isotropic film with thermal conductivity equal to the geometric mean of the film conductivity parallel to and perpendicular to the film surface, and an equivalent film thickness modified by thermal anisotropy. The identification of a dimensionless interfacial thermal resistance involving the dimensions of the heated area on the film surface shows that, as expected, the effect of the film/substrate interfacial thermal resistance is more prominent in thin films (proximity of film/substrate interface to the heated area on the film surface).

The apparent thermal conductivity of the coated substrate consists of contributions due to the film, the film/substrate interface, and the substrate itself. In the limiting case of thin, thermally-insulating films and interfaces of low thermal resistance, we specifically showed that the total thermal resistance of the coated substrate is the sum of the resistances of the film, the film/substrate interface, and the substrate. This result allows the extraction of the intrinsic film thermal conductivity and the interface thermal resistance from the experimentally-measured dependence of the effective film thermal conductivity on film thickness. The measured thickness dependence of thin film conductivity is well described in terms of such a film/substrate interface thermal resistance.

At the microstructural level, we considered the effect of porosity along the film/substrate interface in increasing the local temperature, and we identified the effects of grain shape in producing an interfacial thermal resistance. In this model, the interface is diffuse and extends over a region encompassing the interface voids, and the interfacial thermal resistance is then viewed as proportional to the temperature drop over the diffuse interface dimensions. Typical void geometries produce an interfacial thermal resistance of approximately the same order of magnitude as those measured experimentally. The effect of porosity within the film itself, in the form of porosity within film grains and inter-columnar thermal resistance across grain boundaries, was also examined and shown to lead to significant anisotropy in the film thermal conductivity parallel to and perpendicular to the film surface.

The approach adopted in this paper uses the heat conduction equation to solve for the temperature profile at the film or film grain levels. Still, for the heat conduction equation to apply (*i.e.* heat flux propor-

tional to temperature gradient), the phonon mean-free-path must be smaller than any other linear dimension governing the problem geometry. The majority of optical films deposited by methods such as sputtering, CVD, physical deposition, etc. are amorphous or glassy (Henager and Pawlewicz [36]; Lambropoulos *et al.* [1]; Carpenter [5]; Griffin *et al.* [21, 22]). Thus, the mean-free-path is of the order of atomic spacing, validating the use of the heat conduction equation. Still, for crystalline dielectric thin films one must consider the effects of phonon scattering [43] from impurities, faults, and geometric boundaries, as discussed by Majumdar in the context of thin films [68].

Acknowledgements

We acknowledge the financial support from Eastman Kodak Company (Rochester, N.Y.), from the National Science Foundation (Grant MSM-8857096), and the Office of Naval Research (Grant N-00014–87-K-0488). We also acknowledge many helpful discussions with Dr. Brain Bartholomeusz from Eastman Kodak, Prof. S. D. Jacobs from the Institute of Optics and Laboratory for Laser Energetics, and Prof. S. J. Burns from the Dept. of Mechanical Engineering at the University of Rochester.

References

[1] Lambropoulos, J. C., Jolly, M. R., Amsden, C. A., Sinicropi, M., Diakomihalis, D. and Jacobs, S. D., *J. Appl. Phys.* **66**, 4230 (1989).
[2] Lambropoulos, J. C., Jacobs, S. D., Burns, S. J., Shaw-Klein, L. and Hwang, S.-S., in *Thin-film Heat Transfer: Properties and Processing*, Alam, M. K., *et al.*, Eds. (American Society of Mechanical Engineers, New York, 1991), HTD **203**, p. 21.
[3] Goodson, K. E. and Flik, M. I., *Appl. Mech. Rev.* **47**, 101 (1994).
[4] Duncan, A. B. and Peterson, G. P., *Appl. Mech. Rev.* **47**, 397 (1994).
[5] Carpenter, Jr., J. A., *Proc. SPIE* **2714**, 445 (1996).
[6] Decker, D. L., Koshigoe, L. G. and Ashley, E. J., in *NBS Special Publication 727, Laser Induced Damage in Optical Materials: 1984*, Bennett, H. E., *et al.*, Eds. (Government Printing Office, Washington, DC., 1986), p. 291.
[7] Guenther, A. H. and McIver, J. K., *Thin Solid Films* **163**, 203 (1989).
[8] Maldonado, J. A., *J. Electron. Mater.* **19**, 699 (1990).
[9] Bartholomeusz, B. J., *J. Appl. Phys.* **65**, 262 (1989).
[10] Nakagawa, H., Nakamura, S., Takahashi, M. and Arimoto, A., *Applied Optics* **31**, 4559 (1992).
[11] Evans, K. E. and Nkansah, M. A., *J. Appl. Phys.* **64**, 3398 (1988).
[12] Nkansah, M. A. and Evans, K. E., *J. Appl. Phys.* **67**, 3242 (1990).
[13] Ono, A., Baba, T., Funamoto, H. and Nishikawa, A., *Japanese J. Appl. Phys.* **25**, L808 (1986).
[14] Tai, Y. C., Mastrangelo, C. H. and Muller, R. S., *J. Appl. Phys.* **63**, 1442 (1988).

[15] Saenger, K. L., *J. Appl. Phys.* **65**, 1447 (1989).
[16] Ristau, D. and Ebert, J., *Applied Optics* **25**, 4571 (1986).
[17] Cahill, D. G. and Allen, T. H., *Appl. Phys. Lett.* **65**, 309 (1994).
[18] Brotzen, F. R., Loos, P. J. and Brady, D. P., *Thin Solid Films* **207**, 197 (1992).
[19] Schafft, H. A., Suehle, J. S. and Mirel, P. G. A., in *Proc. IEEE 1989 Int. Conf. on Microelectronic Test Structures* (IEEE, New York, 1989), **2**(1), p. 121.
[20] Touloukian, Y. S., Kirby, R. K., Taylor, R. E. and Lee, T. Y. R., *Thermophysical Properties of Matter: Thermal Conductivity-Nonmetallic Solids* (Plenum Publishing Corporation, New York, 1970), **2**.
[21] Griffin, A. J., Brotzen, F. R. and Loos, P. J., *J. Appl. Phys.* **75**, 3761 (1994).
[22] Griffin, A. J., Brotzen, F. R. and Loos, P. J., *J. Appl. Phys.* **76**, 4007 (1994).
[23] Cahill, D. G., Fischer, H. E., Klitsner, T., Swartz, E. T. and Pohl, R. O., *J. Vac. Sci. Technol.* **A7**, 1259 (1989).
[24] Goodson, K. E., Flik, M. I., Su, L. T. and Antoniadis, D. T., *ASME J. Heat Transfer* **116**, 317 (1994).
[25] Lee, S.-M., Cahill, D. G. and Allen, T. H., *Phys. Rev.* **B52**, 253 (1995).
[26] Kuo, B. S. W., Li, J. C. M. and Schmid, A. W., *Appl. Phys.* **A55**, 289 (1992).
[27] Kuo, B. S. W. and Schmid, A. W., *J. Appl. Phys.* **74**, 5159 (1993).
[28] Matsumoto, D. S., Reynolds, C. L., Jr. and Anderson, A. C., *Phys. Rev.* **B16**, 3303 (1977).
[29] Swartz, E. T. and Pohl, R. O., *Reviews of Modern Physics* **61**, 605 (1989).
[30] Shaw-Klein, L., Burns, S. J. and Jacobs, S. D., in *Electronic Packaging Materials Science*, Lillie, E. D., *et al.*, Eds., Materials Research Society Symposium Proceedings (MRS, Pittsburgh, 1991), **203**, p. 235.
[31] Shaw-Klein, L., Hatwar, T. K., Burns, S. J., Jacobs, S. D. and Lambropoulos, J. C., *J. Mater. Res.* **7**, 329 (1992).
[32] Reichling, M., Wu, Z. L., Welsch, E., Schafer, D. and Matthias, E., in *Photoacoustics and Photothermal Phenomena III*, Bicanic, B., Ed., Springer Series in Optical Sciences (Springer-Verlag, Berlin, 1992), **69**, p. 698.
[33] Wu, Z. L., Kuo, P. K., Wei, L., Gu, S. L. and Thomas, R. L., *Thin Solid Films* **236**, 191 (1993).
[34] Wu, Z. L., Reichling, M., Hu, X.-Q., Balasubramanian, K. and Guenther, K. H., *Applied Optics* **32**, 5660 (1993).
[35] Swimm, R. T., *Proc. SPIE* **1441**, 45 (1990).
[36] Henager, C. H. and Pawlewicz, W. T., *Applied Optics* **32**, 91 (1993).
[37] Powell, R. W., in *Thermal Conductivity*, Tye, R. P., Ed. (Academic Press, New York, 1969), **2**, p. 276.
[38] Movchan, B. A. and Demchishin, A. V., *Phys. Met. Metallogr.* **28**, 83 (1969).
[39] Thornton, J. A., *J. Vac. Sci. Technol.* **11**, 666 (1974).
[40] Thornton, J. A., *Ann. Rev. Mat. Sci.* **7**, 239 (1977).
[41] Messier, R., *J. Vac. Sci. Technol.* **A4**, 490 (1986).
[42] Hagen, S. J., Wang, Z. Z. and Ong, N. P., *Phys. Rev.* **B40**, 9389 (1989).
[43] Klemens, P. G., in *Solid State Physics*, Seitz, F. and Turnbull, D., Eds. (Academic Press, New York, 1958), **7**, p. 1.
[44] Reissland, J. A., *The Physics of Phonons* (John Wiley, London, 1973), p. 117.
[45] Shaw-Klein, L. J., in LL E Review (Laboratory for Laser Energetics, Rochester, N.Y., October/December, 1991), **49**, pp. 24–40.
[46] Carslaw, H. S. and Jaeger, J. C., *Conduction of Heat in Solids* (Oxford University Press, London, 1959), Chap. VIII, p. 216.
[47] Dryden, J. R., *ASME J. of Heat Transfer* **105**, 408 (1983).
[48] Oberhettinger, F., *Tables of Bessel Transforms* (Springer Verlag, New York, 1972), entry 2.9, p. 7.
[49] Gradshteyn, I. S. and Ryzhik, I. M., *Table of Integrals, Series, and Products: Corrected and Enlarged Edition*, trans. by Jeffrey, A. (Academic Press, New York, 1980), entry 6.575.2, p. 693.

[50] Majumdar, A. and Tien, C. L., *ASME J. Heat Transfer* **113**, 516 (1991).
[51] Ogden, T. R., Rathsam, A. D. and Gilchrist, J. T., *Mat. Lett.* **5**, 84 (1987).
[52] Stark, I., Stordeur, M. and Syrowatka, F., *Thin Solid Films* **226**, 185 (1993).
[53] Shaw-Klein, L. J., Burns, S. J., Kadin, A. M., Jacobs, S. D. and Mallory, D. S., *Supercond. Sci. Technol.* **5**, 368 (1992).
[54] Yang, B., Walden, B. L., Messier, R. and White, W. B., *Proc. SPIE* **821** 68 (1987).
[55] Dubost, L., Rhallabi, A., Perrin, J. and Schmitt, J., *J. Appl. Phys.* **78**, 3784 (1995).
[56] Thornton, J. A., *Proc. SPIE* **821**, 95 (1987).
[57] Mazor, A., Srolovitz, D. J., Hagan, P. S. and Bukiet, B. G., *Proc. SPIE 821* **88** (1987).
[58] Maxwell, J. C., *A Treatise on Electricity and Magnetism* (Clarendon Press, Oxford, 1904), p. 435.
[59] Brailsford, A. D. and Major, K. G., *Brit. J. Appl Phys.* **15**, 313 (1964).
[60] Hashin, Z. and Shtrikman, S., *J. Appl. Phys.* **33**, 3125 (1962).
[61] Budiansky, B., *J. Composite Materials* **4**, 286 (1970).
[62] Schulz, B., *High Temperature-High Pressure* **13**, 649 (1981).
[63] Reynolds, J. A. and Hugh, J. M., *Proc. Phys. Soc.* **B70**, 769 (1957).
[64] Rocha, A. and Acrivos, A., *Quart. J. Mech. Appl. Math.* **26**, 217 (1972).
[65] Rocha, A. and Acrivos, A., *Quart. J. Mech. Appl. Math.* **26**, 441 (1973).
[66] Redondo, A. and Beery, J. G., *J. Appl. Phys.* **60**, 3882 (1986).
[67] Miloh, T. and Benveniste, Y., *J. Appl. Phys.* **63**, 789 (1988).
[68] Majumdar, A., *ASME J. Heat Transfer* **115**, 7 (1993).